

Preparation of modified hollow glass microspheres using Fe₂O₃ and its flame retardant properties in thermoplastic polyurethane

Chuanmei Jiao¹ · Li Zhao¹ · Xilei Chen¹

Received: 14 May 2016 / Accepted: 4 September 2016 / Published online: 20 September 2016
© Akadémiai Kiadó, Budapest, Hungary 2016

Abstract In this paper, the hollow glass microspheres coated with Fe₂O₃ (HGM-Fe₂O₃) were synthesized and characterized by scanning electron microscopy (SEM–EDS) and X-ray photoemission spectroscopy, respectively. Then, the flame retardant and smoke suppression properties of HGM-Fe₂O₃ in thermoplastic polyurethane (TPU) composites have been investigated intensively using several methods, including cone calorimeter test (CCT), smoke density test (SDT), scanning electron microscopy, and thermogravimetric analysis/infrared spectrometry. The CCT results showed that HGM-Fe₂O₃ can greatly enhance the flame retardance of polymer matrix materials compared with TPU. For example, HGM-Fe₂O₃ can reduce heat release rate, total heat release, and smoke release of TPU composites in the combustion process. The SDT results showed that HGM-Fe₂O₃ can effectively decrease the amount of smoke production in the test. Furthermore, the TG results indicate that HGM-Fe₂O₃ can decrease the initial decomposition temperature, and change the structure of char residue layer.

Keywords Hollow glass microspheres · Fe₂O₃ · Thermoplastic polyurethane · Flame retardant

Introduction

Thermoplastic polyurethane (TPU) is one of the most versatile engineering thermoplastics with elastomeric properties [1–5], which is a linear alternating copolymer

consisting of hard and soft segments. Because of its excellent physical properties, chemical resistance, abrasion resistance, and good adhesion, TPU has been widely used in coatings and films, automotive, offshore, and infrastructure cables [6, 7]. Unfortunately, its applications have greatly been limited by its inherent flammability and smoke formation. Therefore, it is important to improve flame retardant and smoke suppression of TPU.

In traditional, flame retardant contained the halogen, products will harm to people in the course of used [8, 9], so the demands for halogen-free flame retardants have become more and more important [10, 11]. Intumescent flame retardant based on nitrogen is environmentally friendly widely used in the TPU composites [12]. But the amount of intumescent flame retardant is usually relatively large which has a great influence on mechanical properties. Inorganic nano-materials used as flame retardants added into polymer materials also have a good retardation effect, and nanocomposite (montmorillonite, clay, nano-ZnO) is widely used in flame retardance of polymer [13–15]. But the nano-material is agglomerated and can aging easily in the process of preparation and application. The controlling of nanoparticle agglomerates is difficult. Should we believe to find a series of material not easy to agglomerates but has small size as flame retardant?

Hollow glass microspheres (HGMs) have attracted considerable interest in the past few decades, because it has excellent physical such as well-defined morphology, uniform size, strong filling ability, low density, and large surface area, small and well-distributed internal stress in products. As a result, HGMs are widely used in industry [16, 17]. HGMs were often used to reinforce polymer for its high compression strength and good fluidity. In our previous work, it has been found HGM has been used as a flame retardant synergism to improve the flame retardant

✉ Xilei Chen
xilei_chen@foxmail.com

¹ College of Environment and Safety Engineering, Qingdao University of Science and Technology, Qingdao 266042, Shandong, People's Republic of China

efficiency and smoke suppression effect in TPU composites based on APP [17, 18]. Because the HGM has the characteristic of low density, the migration of HGM onto the surface of the sample when the composites in the melt stage, which could have been a barrier from the flame zone to the underlying materials, restrained the flammable gases to the flame zone [19, 20]. And can HGM be used as flame retardant alone? HGM may be used effective flame retardants for the polymer with high charring yield property. HGM can migrate onto the surface of the sample, which can change the structure of char residue in the cone calorimeter test [21]. There are a large number of hydroxyl groups on the surface of HGM, which could be modified using metal oxides, such as including Fe_2O_3 . Furthermore, Fe_2O_3 can be used as flame retardant synergism [22] and smoke suppression agents [23] in polymer composites. So, a new flame retardant could be obtained combining Fe_2O_3 with HGM.

In this paper, HGM- Fe_2O_3 was successfully synthesized by modifying HGM with Fe_2O_3 and characterized by SEM-EDS and XPS, respectively. Then, the flame retardant and smoke suppression properties of HGM- Fe_2O_3 in TPU composites were intensively investigated using SDT, CCT, and TG-IR.

Experimental

Materials

Commercial TPU (9380A) was produced by Bayer, German. The basic properties of TPU are as follows, density: 1.110 g cm^{-3} (ISO1183); hardness: 82A (ISO868); tensile strength: 40 MPa (ISO527-1,-3); elongation at break: 500 % (ISO527-1,-3). HGM was produced the PQ corporation (grade 5020, particle size of 5–115 μm , medium particle of 55 μm , density of 0.2 g cm^{-3}). $\text{FeCl}_3 \cdot 6\text{H}_2\text{O}$ was purchased from the Sinopharm Chemical Reagent Co., Ltd.

Synthesis of HGM- Fe_2O_3

HGMs were cleaned by pure water rinse for 5 min, in 10 % sodium hydroxide solution for corrosion with supersonic clean for 30 min, rinsed with pure water for four times, and then put that in a vacuum oven at $80 \text{ }^\circ\text{C}$ for 2 h. Ethanol (150 mL) and water (100 mL) were added in turn to flask containing HGM (8 g) at $70 \text{ }^\circ\text{C}$, with uniform stirring. FeCl_3 solution (1 %, 30 mL) and sodium hydroxide solution (1 %, 30 mL) were slowly dropped to the flask at the same time, maintaining the pH value of 6.0 for 5 h. The product has been obtained after dried in a vacuum oven at $80 \text{ }^\circ\text{C}$ for 6 h, and the modified HGMs are moved to in a vacuum furnace at $500 \text{ }^\circ\text{C}$ for 2.0 h.

Preparation of samples

The TPU pellets were dried at $80 \text{ }^\circ\text{C}$ for 4 h. A certain amount of TPU was melted in the mixer at $175 \text{ }^\circ\text{C}$. Then a certain amount of HGM or HGM- Fe_2O_3 was added into the mixer. Later, the samples were hot-pressed at about $180 \text{ }^\circ\text{C}$ under 10 MPa for 20 min into sheets of suitable thickness for analysis. Formulations of flame retardant TPU composites: TPU-0 is composed by pure TPU, TPU-1 is composed by 99.5 mass% TPU and 0.5 mass% HGM, TPU-2 is composed by 99.5 mass% TPU and 0.5 mass% HGM- Fe_2O_3 .

Measurements

X-ray photoemission spectroscopy (XPS)

The XPS spectra were recorded with a VG Escalab mark II spectrometer (VG Scientific Ltd., UK), using Al K α excitation radiation ($h\nu = 1253.6 \text{ eV}$) and calibrated by assuming the binding energy of carbonaceous carbon to be 284.6 eV .

Scanning electron microscopy (SEM)

Scanning electron microscopy (SEM) studies were performed using a Hitachi X650 scanning electron microscope.

Cone calorimeter

The cone calorimeter (Stanton Redcroft, UK) tests were performed according to ISO 5660 standard procedures. Each specimen of dimensions $100 \times 100 \times 3 \text{ mm}^3$ was wrapped in aluminum foil and exposed horizontally to an external heat flux of 35 kW m^{-2} .

Smoke density test

A smoke density test machine JQMY-2 (Jianqiao Co., China) was used to measure the smoke characteristics according to ISO 5659-2 (2006). Each specimen of dimensions $75 \times 75 \times 2.5 \text{ mm}^3$ was wrapped in aluminum foil and exposed horizontally to an external heat flux of 25 kW m^{-2} with or without the application of a pilot flame.

Thermogravimetric analysis

Thermogravimetric analysis (TG) of the sample was performed using a DT-50 (Setaram, France) instrument. About 10.0 mg of sample was put in an alumina crucible and heated from ambient temperature to $700 \text{ }^\circ\text{C}$. The heating rates were set as between 5 and $20 \text{ }^\circ\text{C min}^{-1}$ (nitrogen atmosphere, flow rate of 60 mL min^{-1}).

Thermogravimetric analysis/infrared spectrometry (TG-IR)

Thermogravimetric analysis/infrared spectrometry (TG-IR) of the sample was performed using a DT-50 (Shimadzu, Japan) instrument that was interfaced to a Varian 2000 FTIR spectrometer. About 10.0 mg of the TPU sample was put in an alumina crucible and heated from 260 to 700 °C. The heating rate was set as 20 K min⁻¹ (nitrogen atmosphere, flow rate of 60 mL min⁻¹).

Results and discussion

Characterization of HGM-Fe₂O₃

The results of XPS show that there exist two iron compound peaks at 711 and 730 eV by the comparison between the two curves as shown in Fig. 1; the analytical results of the chemical elements from the material of the HGM-Fe₂O₃ are that 1.89 % of iron as shown in Fig. 2a. It is clear that the iron elements content on HGM-Fe₂O₃ surface (0.99 %) is higher than that of pure HGM surface (0 %). Figure 2b shows the photographs of HGM and HGM-Fe₂O₃. According to the comparison between photographs, it can be seen that they were very different. For HGM, there is nothing in the surface. For HGM-Fe₂O₃, there is film layer on the surface.

Cone calorimeter test

Heat release rate (HRR)

The heat release rate (HRR) versus time curves for the samples is shown in Fig. 3. TPU-0 is a readily flammable polymeric material, and a sharp peak HRR (PHRR) of 1517 kW m⁻² is obtained at 195 s, the PHRR value of

TPU-1 is 1591 kW m⁻² at 220 s, and the PHRR value of TPU-2 is 885 kW m⁻² at 220 s. The PHRR value of TPU-2 decreased significantly compared with TPU-0, and it is strange that the PHRR value of TPU-1 is slightly larger. It should be noted that HGM had no flame retardant effect but the modified HGM (HGM-Fe₂O₃) had the obviously flame retardant effect that reduces the heat release rate when the sample with the addition 0.5 mass% HGM-Fe₂O₃. The above phenomenon can be explained by the compact char residue formed on the surface of sample in cone calorimeter test. The time to ignition (TTI) of pure TPU was the shortest among all samples, and the reason may be due to the samples (TPU-1 and TPU-2) isolated partial heat and decrease to produce combustible gas compared with TPU-0. Thermoplastic polyurethane can be softened by heat; then, HGM or HGM-Fe₂O₃ can migrate progressively onto the surface of the sample [17]. When the TPU composite burns, HGM onto the surface can form dense protrusion and play a role of a wick, "Candlewick" meaning that a candle burning needed wick. The process of polymer melt flowing along wick to the high-temperature region will promote the burning [24]. The modified HGMs have no effect as a wick, we think this is a link to iron compound from surface of HGM, and the flame retardation and smoke suppression effect of iron compounds have been confirmed [25]. The cone calorimeter is based on side heating by infrared thermal radiation. The samples were heated from the upper side. The accumulated HGM consequently formed a charred layer acts as a heat insulation barrier. This charred layer prevented heat transfer and transportation of degraded products between polymer and surface, thus reduced the HRR.

Total heat release (THR)

Figure 4 presents the THR for all of the samples. The slope of the THR curve is assumed to be representative of flame spread [26]. It can be seen the THR of TPU-0 is higher than the samples with HGM or HGM-Fe₂O₃. The flame spread of TPU-0 is faster than samples with HGM or HGM-Fe₂O₃ (TPU-1 or TPU-2) in the time range between 50 and 180 s. After 180 s, the slope of TPU-1 was increased, and it is clearly that the slope remained remarkably low when the sample with HGM-Fe₂O₃, which is conducive to prevent the spread of fire. The results show that the flame spread of pure TPU is quickly in the earlier stage. In the case of the samples with HGM and HGM-Fe₂O₃, the heat insulation of HGM and HGM-Fe₂O₃ can be obtained during the combustion process, which results in the low THR. Furthermore, there is the lowest THR for TPU-2 because of the Fe₂O₃ on the surface of HGM.

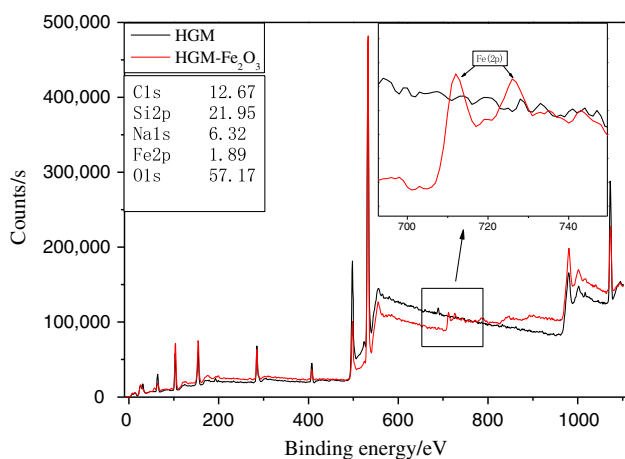


Fig. 1 XPS results of HGM and HGM-Fe₂O₃

Fig. 2 EDS (a) and SEM (b) image results of HGM and HGM-Fe₂O₃

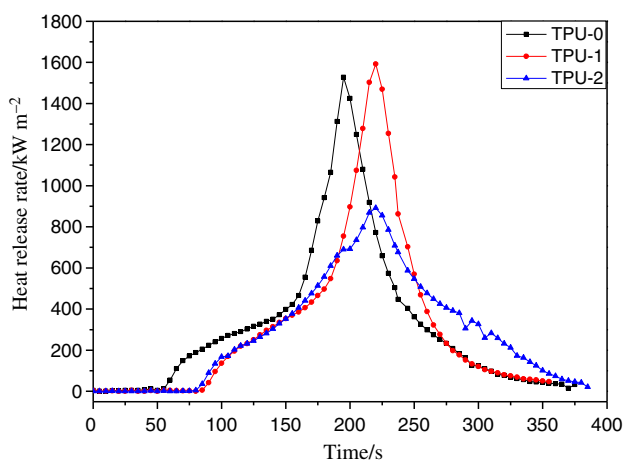
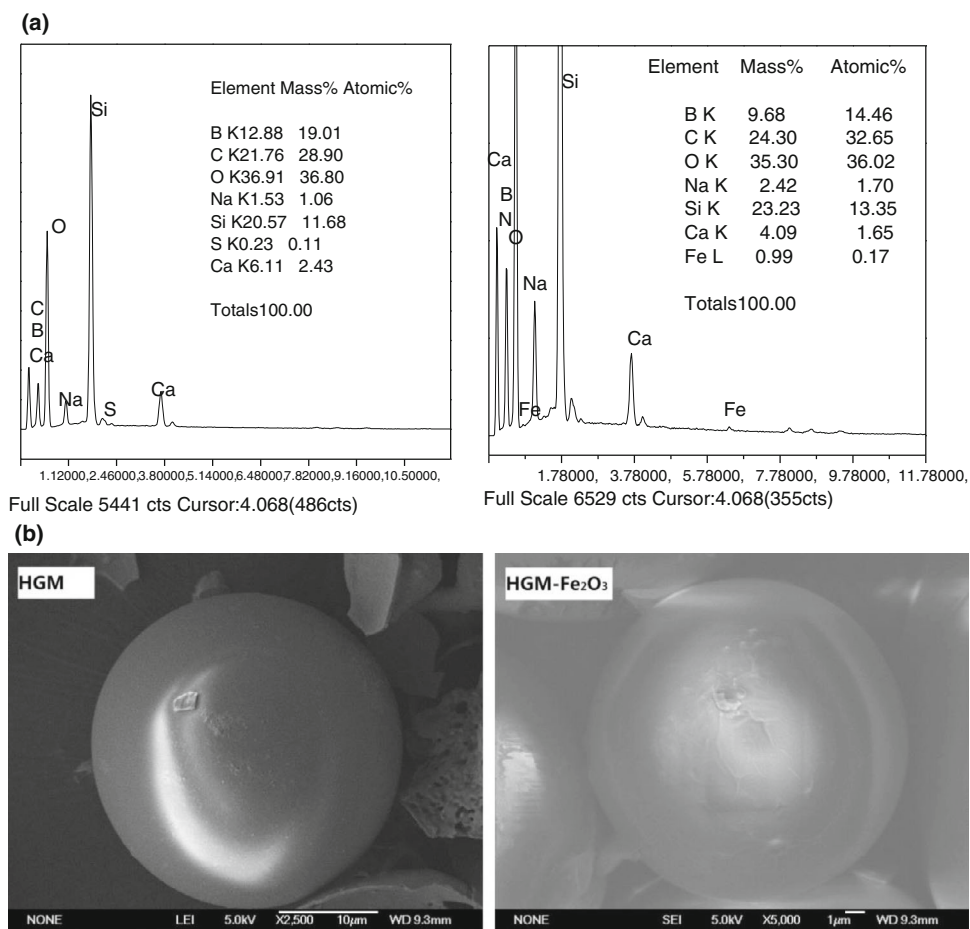


Fig. 3 Heat release rate curves of flame retardant TPU composites at flux of 35 kW m⁻²

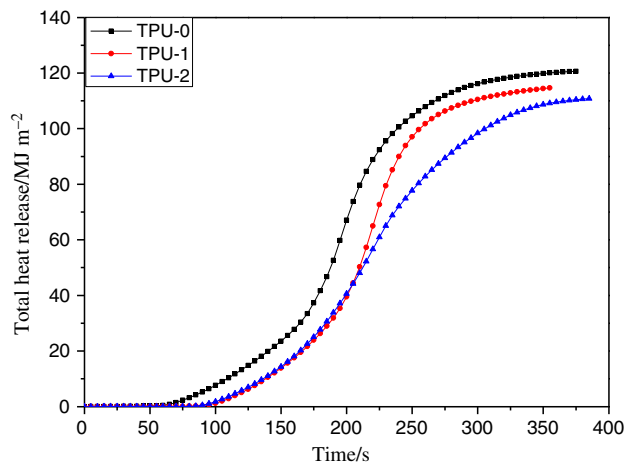


Fig. 4 Total heat release rate curves of flame retardant TPU composites at flux of 35 kW m⁻²

Mass

Figure 5 presents the Mass curves of the samples. It can be seen that the mass loss of the samples with HGM and HGM-Fe₂O₃ (TPU-1 and TPU-2) is lower than that of TPU-0 without any additive. This result can be used to illustrate why the ignition time of TPU-0 is shorter than those of TPU-1 and TPU-2. Furthermore, the mass loss of TPU-0 is larger than those of TPU-1 and TPU-2 during the combustion process, which means there is much larger amount of volatile compounds formed. Combining the results from Figs. 3 and 4, the volatiles compounds are mainly flammable gases. The reason for the low mass loss for TPU-1 and TPU-2 is that both HGM and HGM-Fe₂O₃ can help to change the structure of char residue layer. On the one hand, both HGM and HGM-Fe₂O₃ can make the char residue compact; on the other hand, both HGM and HGM-Fe₂O₃ can migrate onto the surface of the samples during the heat process and show good barrier effect for heat and mass transferring. It should be figured out that the mass loss of TPU-2 with HGM-Fe₂O₃ is much lower than that of HGM from 180 to 300 s. After that, the mass loss of TPU-2 is larger than that of TPU-1. This can be illustrated that Fe₂O₃ on the surface of HGM-Fe₂O₃ can promote the carbonization of TPU to form char residue layer. Then, the char residue is unstable and can be oxidized in the conditions with high temperature and oxygen, leading low char residue for the sample with HGM-Fe₂O₃.

Smoke production rate (SPR)

Smoke performance of flame retardant material is a very important parameter in fire safety fields. The incomplete combustion of flame retardant composite systems can be seen in the smoke production rate. The smoke production

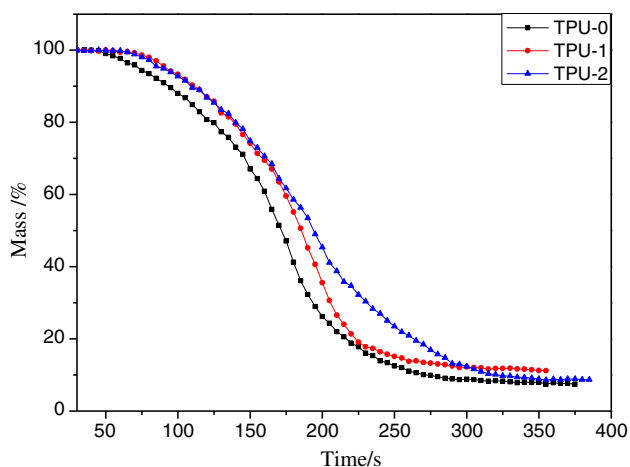


Fig. 5 Mass loss curves of flame retardant TPU composites at a flux of 35 kW m⁻²

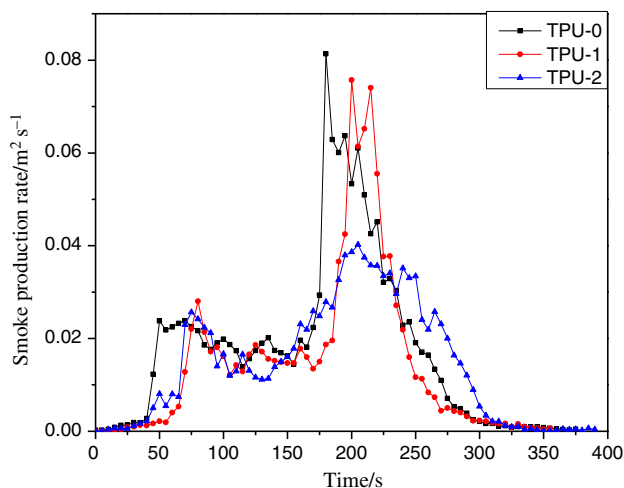


Fig. 6 Smoke production rate curves of flame retardant TPU composites at flux of 35 kW m⁻²

rate (SPR) curves of TPU composites are given in Fig. 6. Compared with the peak SPR values of TPU-0 (0.081 m² s⁻¹) and TPU-1 (0.076 m² s⁻¹), the peak SPR value of TPU-2 is 0.040 m² s⁻¹, which is the lowest one among all samples. The peak SPR value decreases greatly with the addition of HGM-Fe₂O₃, and the smoke suppression effect of HGM-Fe₂O₃ is more obvious than that of HGM. Iron(III) compound as effective smoke suppressant can reduce smoke production when the polymer composites are burning, and in some polymer blends this compound was found to reduce smoke production by up to 50 % (in some cases reductions of 65 % were recorded) while reducing the flammability of the blends [25, 27]. And it can be seen that the time to the peak SPR value of TPU-0 is earlier than that of TPU-1 or TPU-2. The peak SPR of TPU-0 appears at 180 s during combustion process, and peak SPR of TPU-1 and TPU-2 appears at 205 and 210 s, respectively. This is corresponding to the TTI of the samples referred to in paragraph HRR above (Fig. 3). Smoke suppression by HGM-Fe₂O₃ can be explained as follows: HGM-Fe₂O₃ can migrate onto the surface of TPU-2, which can improve the stability of the char residue layer, protecting the inner matrix, and reduce the amount of combustible gas and smoke-forming materials in the gas phase during combustion, because of the Fe₂O₃, the char layer denser and fairly rigid.

Total smoke release (TSR)

Figure 7 presents the total smoke release (TSR) curves of the samples. It can be seen that the TSR of TPU-1 with HGM is much lower than that of TPU-0 before 300 s. This can be illustrated that HGM can change the structure of char residue from TPU-1 in the combustion process, which results in less smoke particulates released. After 300 s, the

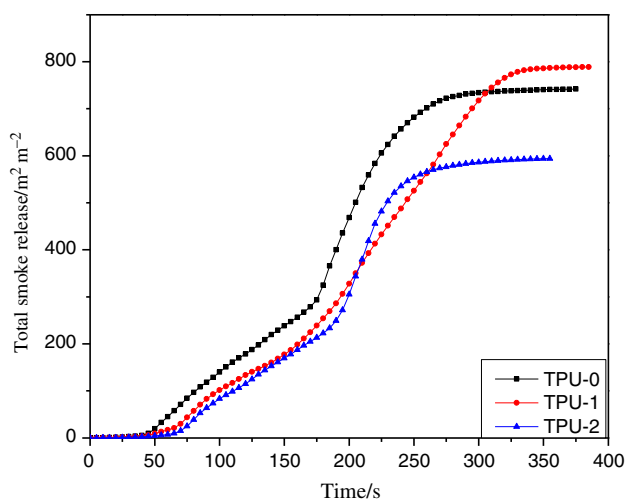


Fig. 7 Total smoke release curves of flame retardant TPU composites at flux of 35 kW m^{-2}

TSR of TPU-1 is larger than that of TPU-0, which is attributed to the fact of the rupture of char residue layer. In the case the sample with HGM- Fe_2O_3 , TPU-2 has a low TSR compared with TPU-1 during 50–200 s, and the TSR value from TPU-2 is much lower than that of TPU-1 at the end of cone calorimeter test. These are the smoke suppression effect of Fe_2O_3 on the surface of HGM- Fe_2O_3 . It has been reported that the iron can help to change and structure of char residue layer that restrains the heat release and smoke generation [28].

Smoke factor (SF)

Figure 8 gives the smoke factor (SF) curves for all samples. SF is the product of HRR and TSR [29]. SF values described the hazards of fire by the aspect of heat and smoke. The peak SF values for all samples (TPU-0 to TPU-2) are 1129, 947, 698 kW m^{-2} , respectively. It can be concluded HGM can reduce the fire hazards of TPU composites. And HGM- Fe_2O_3 can further decrease the fire hazards of TPU composites, including heat (Fig. 3) and smoke (Fig. 6). So, HGM- Fe_2O_3 can be used as effective flame retardant and smoke suppression agent for TPU resin.

Photographs of char residue

Figure 9 shows the photographs and SEM graphs of char residues after the cone calorimeter tests (CCTs). A carbonaceous char formed during expansion can act as a thermal shield between the flame zone and the substrate, preventing heat from penetrating [30]. It can be seen that there are many holes on the surface of carbon layer from TPU-0 sample. This structure cannot effectively bind

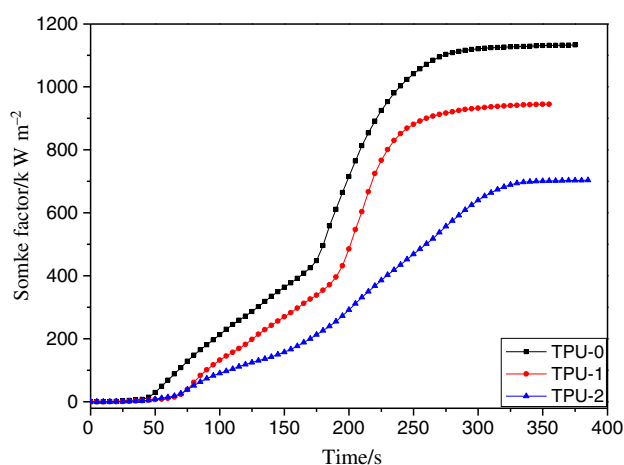


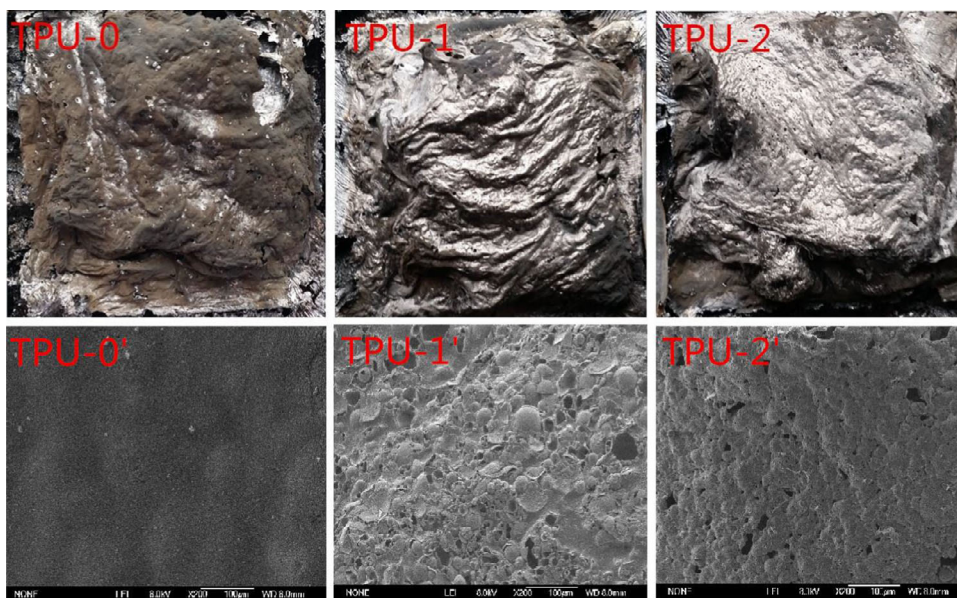
Fig. 8 Smoke factor curves of flame retardant TPU composites at flux of 35 kW m^{-2}

combustible gas and smoke particulates from the underlying materials, which resulting high heat release rate and smoke production rate. For TPU-1 sample, there is a char residue film formed on the surface of the sample at first glance. However, there are many micro-holes, which can release flammable gases into flame zone, resulting high heat release rate. But a lot of smoke particulates cannot pass through the micro-holes and were bounded in the solid phase during combustion process. This would lead less smoke release [31]. For the sample with HGM- Fe_2O_3 , the char residue layer structure is not dense and smooth. This result cannot be used to illustrate the HRR and SPR results.

The SEM images displayed the different surface morphologies between TPU-1 and TPU-2. For TPU-2', the char residue image shows a compact appearance and smooth surface, HGM- Fe_2O_3 on inner of the surface. Compared with TPU-2', the surface of TPU-1' appears a significant uplift phenomenon, the result of extensional fracturing of the char residue surface structure due to longitudinal compression warping deformation. It is clear that compared with HGM char residue structure, HGM- Fe_2O_3 has better thickness and mechanical strength. On the other hand, there are many holes in the surface of TPU-1 (TPU-1') sample, and there are many crevices in the surface of TPU-0 (TPU-0') sample. In contrast, the char residue of TPU-2 (TPU-2') shows a compact appearance and smooth surface. Holes and crevices are nearly not existed in the char residue of TPU-2. This can be explained that HGM- Fe_2O_3 can help to promote charring and change the structure of carbon layer, forming compact carbon layer.

However, the mass results in Fig. 5 can be combined with the structure of char residue after cone calorimeter test. From Fig. 5, it has been concluded that Fe_2O_3 can promote carbonization of TPU in the time between 180

Fig. 9 Photographs of flame retardant TPU composites after cone calorimeter test



and 300 s. At the same time range, the low HRR and SPR are also gotten. It can speculate that there is much dense char residue layer formed on the surface of TPU-2. But the char residue is unstable, which can be oxidized with high temperature and oxygen. So, the photographs from Fig. 9 after cone calorimeter test could not be used to explain the flame retardant and smoke suppression properties for TPU-2 [28].

Fire performance index (FPI) and fire growth index (FGI)

In order to judge the hazards of fire more clearly, the fire performance index (FPI) and the fire growth index (FGI) are calculated after CCT [32, 33]. The FPI is defined as the ratio of time from ignition to PHRR, and the FGI is defined as the ratio of peak HRR to time to PHRR [34]. From Fig. 10, it can be seen that the FPI values increase and the FGI values decrease compared pure TPU with the addition of HGM-Fe₂O₃; both the FPI values and the FGI values decrease with the addition of HGM-Fe₂O₃. HGM-Fe₂O₃ can extend the time of reach crashing and reduce the risk of

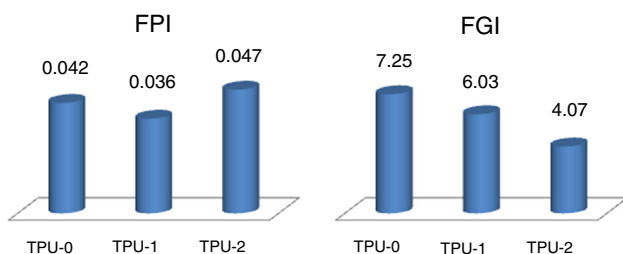


Fig. 10 Fire performance index for flame retardant TPU blends at a flux of 35 kW m⁻²

fire, which indicates the samples with HGM-Fe₂O₃ have good flame retardancy.

Smoke density test

The luminous flux curves of TPU composites are presented in Fig. 11 in the smoke density test without (a) and with (b) flame. It can be seen from Fig. 11a. The luminous flux of TPU-0 gradually reduced and reached 12.1 % at 1200 s. The luminous flux of TPU-1 is lower than that of the TPU-0 in the initial 500 s, which is attributed to the fact HGM with low thermal conductivity leads the temperature on the surface of the material to increase rapidly, resulting much volatile compounds (including smoke particulates) formed quickly. This would decrease the luminous flux value of TPU-1. At the same time, HGM migrated and aggregated on the surface of the sample, and change the structure of char residue to compact, which could be act as barrier for heat from outside and smoke particulates from underlying materials. So, the luminous flux of TPU-1 is higher than that of the TPU-0 after 500 s. In the case of TPU-2 sample with HGM-Fe₂O₃, the luminous flux further decreased compared with TPU-1 with HGM in the initial 200 s. This can be illustrated that Fe₂O₃ on the surface of HGM-Fe₂O₃ can catalyze TPU decomposing to form flammable gases, smoke particulates, and carbon char residue. The smoke particulates formed at low temperature decreased the luminous flux of TPU-2. Then, the char residue layer act as barrier for heat and mass transferring. Also, there is an important reason that HGM-Fe₂O₃ can improve the char residue mass, which means the amount of volatile

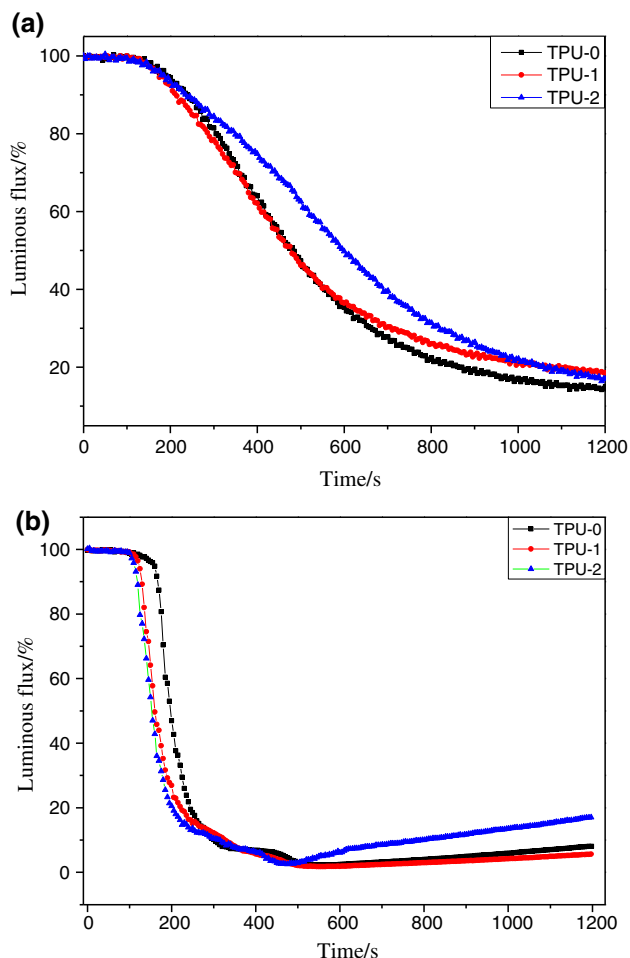


Fig. 11 Luminous flux curves of TPU composites without (a) or with (b) flame

compounds become little, especially for the content of smoke particulates.

From Fig. 11b, it can be seen that the luminous flux of all samples decreased rapidly between 100 and 300 s. The luminous flux values of the samples with HGM and HGM-Fe₂O₃ decreased at short time. And the luminous flux value of TPU-2 is lower than that of TPU-1 before 400 s. This means there are a large amount of smoke particulates formed induced by flame. After 450 s, the luminous flux values of all samples increased, which is attributed to the aggregation and settlement of smoke particulates.

Thermogravimetric analysis (TG)

Figure 12 shows the TG curves for all samples. The initial decomposition temperature of TPU-0, TPU-1, and TPU-2 is 330, 303 and 295 °C (5.0 mass% mass loss), respectively. It is shown that HGM and HGM-Fe₂O₃ can promote

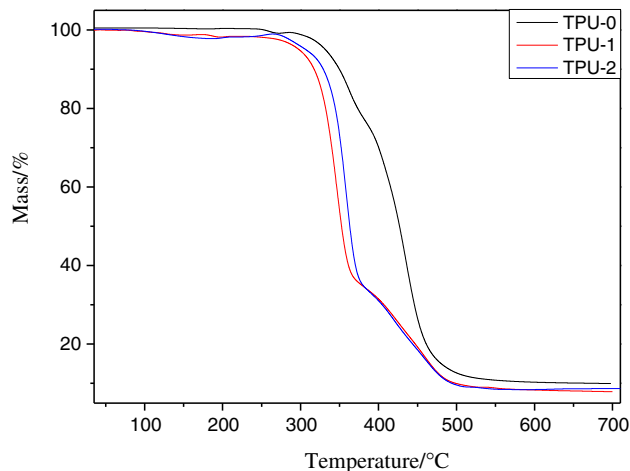


Fig. 12 TG curves of flame retardant TPU composites at a constant heating rate of 10 K min⁻¹

the degradation of TPU at low temperature. When the temperature is raised to 700 °C, the amounts char residue of TPU-0, TPU-1, and TPU-2 were 10.3, 8.5, and 8.9 %, respectively. The DTG curves are given in Fig. 13, and the rate of mass loss with temperature for the TPU-1/TPU-2 composites was significantly higher than that for TPU-0 in the first stage. HGM can improve char formation during combustion in composite; even HGM was added to the composites will accelerate the composite system cracking. Experiments show that the production is noninflammable gases associated with cone calorimeter data; the composites brought obvious mass loss before reach TTI without burning. Two stages can be shown in DTG curves. The first peak is the decomposition of hard domains comprising of urethane linkages at 330 °C, and the second peak stands for soft domains. For TPU-1, the first stage stands for a significant drop in mass; the second stage showed the mass

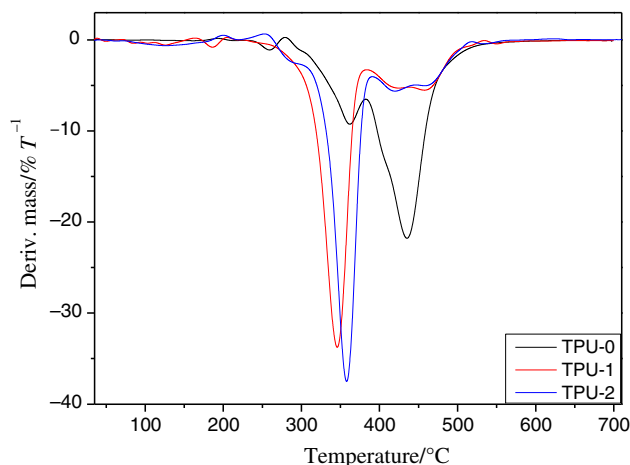


Fig. 13 DTG curves of flame retardant TPU composites at a constant heating rate of 10 K min⁻¹

loss is not as significant as the previous period. In early stage, the increase in the rate of mass loss with temperature for the TPU-1/TPU-2 composites was significantly lower than that for TPU-0, and this is contradicted by mass curve of CCT results. Compared with the DTG results of TPU-1, the TPU-2 peak DTG temperature and maximum mass loss are higher than those of TPU-1. For such cases, we explain from two respects. First, the heating methods of the two instruments are different (CCT uses side heating and TG uses full-circumferential heating). Second, the size of samples is different. Focused by radiation heat in samples surface external, part of the heat to be reflected back due to the HGM has been migrated to the surface. The samples were heated by full-circumferential; the upper HGM cannot play the effectiveness of the insulation. Furthermore, large sample size is easier to form char layer.

TG-IR characterization of volatile products

The volatilized products formed during the thermal degradation of the TPU composites were characterized by TG-IR technique and are shown in Figs. 14–16, respectively. The TG-IR technique that directly gives identification of the volatilized products can significantly contribute to an understanding of thermal degradation mechanisms [35]. In this paper, the investigation on the characterization of the volatilized products by TG-IR instrument was focused on nitrogen atmosphere. It is important to note that peaks in the regions of around 3230–3550, 2800–3150, 2250–2400, 1700–1850, 1250–1500, and 950–1150 cm⁻¹. Some of the volatilized decomposition products of the TPU are unambiguously identified by characteristic strong FTIR signals, such as H₂O (3230–3550 cm⁻¹), CO₂

(2300–2400 cm⁻¹), CO (2250–2300 cm⁻¹), carboxylic acid (1700–1850 cm⁻¹), and aliphatic hydrocarbons (2800–3150, 1250–1500, and 950–1150 cm⁻¹). In the process of depolymerization, the main products of the thermal decomposition of TPU are compounds containing H₂O, CO₂, CO, carboxylic acid, and aliphatic hydrocarbons, etc. The depolymerization processes of these three samples are significantly different according to Fig. 17. In the case of TPU-0, it decomposes drastically with lots of pyrolysis products, and at last, no product released that the composites pyrolyzed completely. In the TPU-1 system, intensity of characteristic peaks CO₂ increases until it reaches the maximum at 460 °C, and then turns into a rapid decrease, and at last, intensity of characteristic peaks of CO₂ is not zero, whereas the decomposition rate of TPU-1 is slowed down. In particular, the decomposition rate of TPU-2 is slowed down further when HGM-Fe₂O₃ is introduced into the TPU composites, because intensity of characteristic peaks of CO₂ is not reaching the peak. In the TPU-1 system, intensity of characteristic peaks of CO appears, and HGM introduced into the TPU composites can produce the poisonous gas (CO) when the composites obtained at higher temperature. It can be observed from the chart above; see that there exit the three FTIR absorption intensity models of the curve. TPU-0 sample in the 400–540 °C range of the intensity peak value is higher; then, the peak value decreased to a lower level at later stage. Similar conditions are to be found in TPU-1 sample, first gradually increased the maximum (about 480 °C) and then began to decreased, in the 400–700 °C range of the intensity peak value is higher, and peak value is still at a high level at later stage. Unlike other sample, the TPU-2 peak value of absorption intensity was gradually increased during increasing with temperature.

Fig. 14 3D FTIR spectra of gas products for TPU-0 at different temperatures

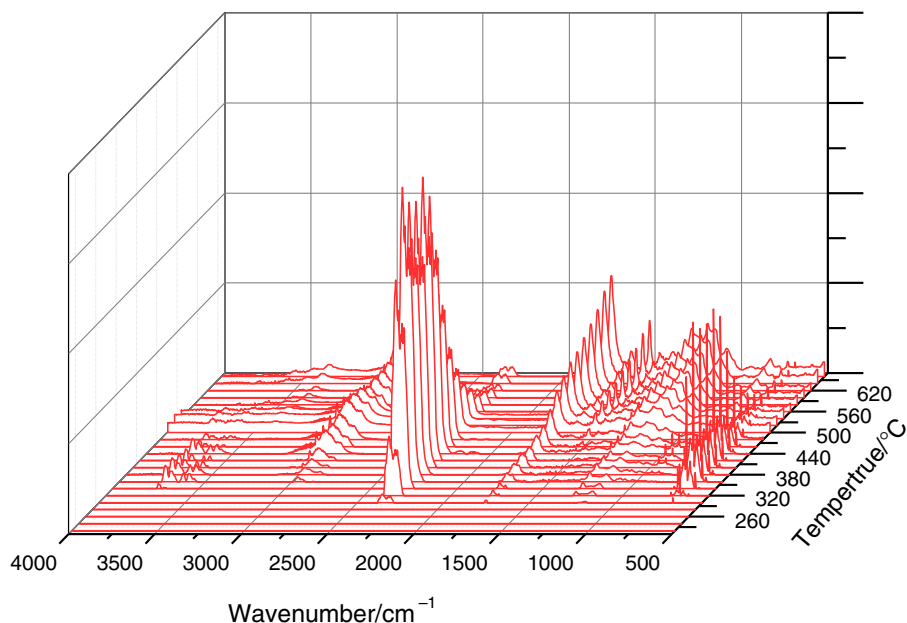


Fig. 15 3D FTIR spectra of gas products for TPU-1 at different temperatures

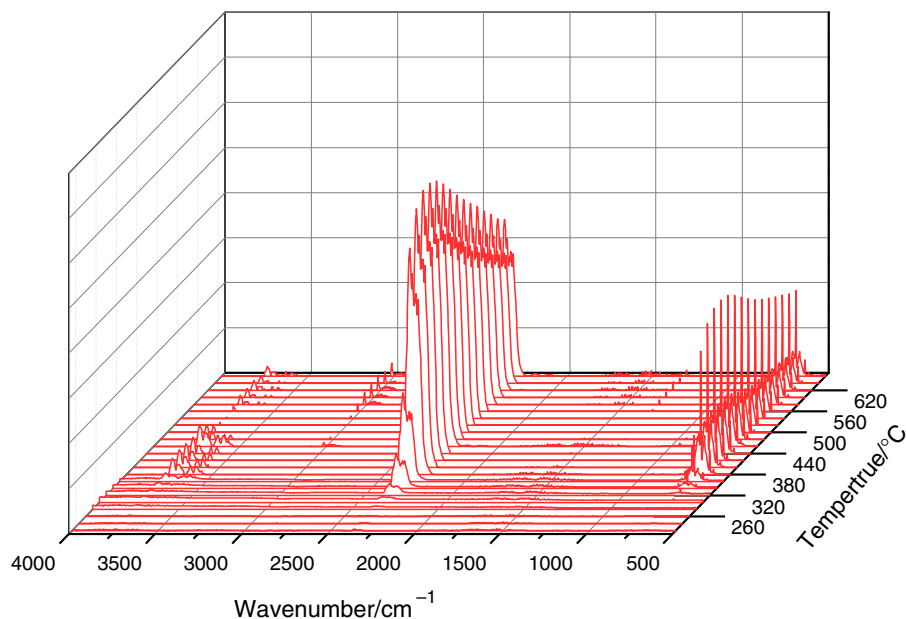
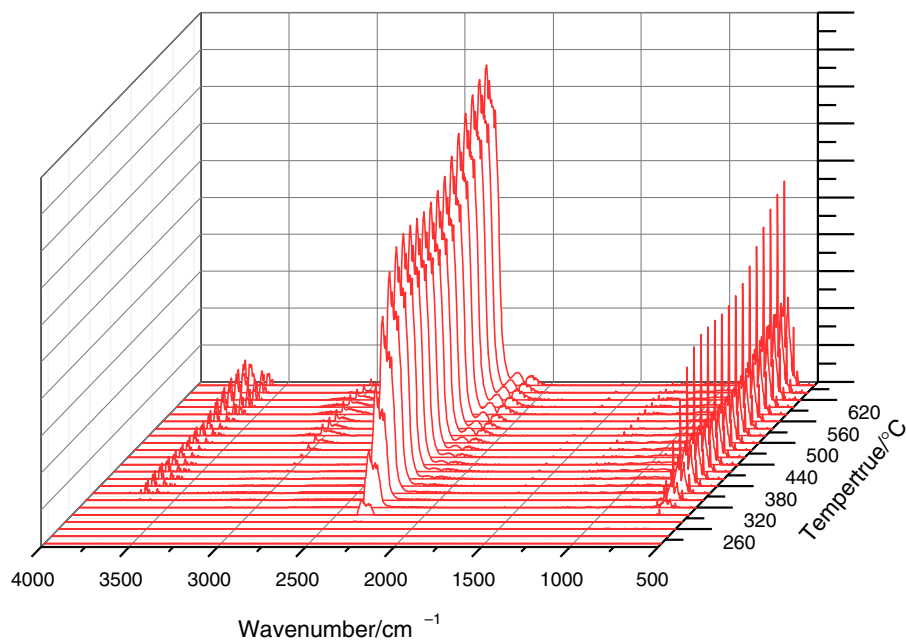


Fig. 16 3D FTIR spectra of gas products for TPU-2 at different temperatures



As shown in Fig. 17a, the decomposition of these three composites does not happen below 260 °C because there is almost no infrared signal under this temperature. The main decomposition products will be detected with the temperature increasing to 320 °C. As for TPU-0, the peak appears at 2960 cm^{-1} indicating the appearance of combustible gas (aliphatic hydrocarbons), due to the rupture of the TPU main chains, which is favorable to combustion. As for TPU-0, the peak appears at 2360 cm^{-1} indicating the appearance of CO_2 . And the intensity of characteristic peaks for CO_2 reaches a maximum with the

temperature increasing to 460 °C (480 °C for TPU-1, 700 °C for TPU-2). This can be illustrated that the sample TPU-0 was decomposed in the first with increasing temperatures, and the first thermal decomposition products CO_2 . Moreover, a maximum signal at 2950 cm^{-1} attributed to aliphatic hydrocarbons can be detected at 500 °C (500 °C for TPU-1, 460 °C for TPU-2). The formation of CO , CO_2 , and aliphatic hydrocarbons is detected, probably due to the rupture of the TPU main chains and the destruction of the C–C and C–O bonds on the main chain [14]. From Fig. 17c, it can be found that, significant peaks

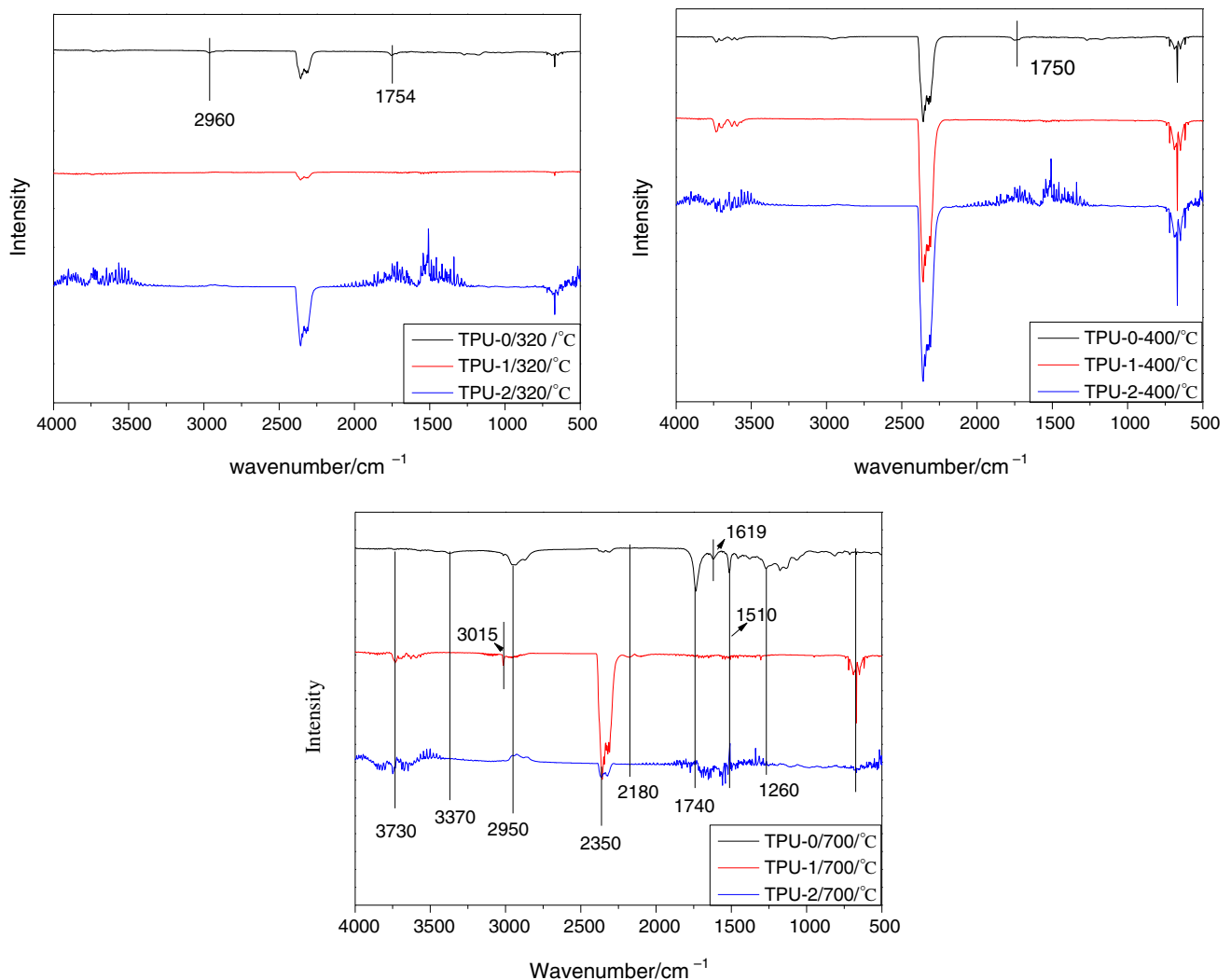


Fig. 17 FTIR spectra of volatilized products during thermal degradation of TPU composites

of CO ($2250\text{--}2300\text{ cm}^{-1}$) at the late stage of thermal degradation, this means that flammable and toxic gases continuously generated. Therefore, it is considered the iron compound surface of HGM can achieve a catalytic effect toward to char layer further to degradation of CO₂. And the sample of unmodified HGM catalyst char layer not only transformed into CO₂, but also there is a certain amount transformed into CO. It is generally known the majority of people who die in fires due to inhale CO. So, the production of CO is dangerous to people.

Conclusions

The CCT results show that HGM-Fe₂O₃ not only greatly reduces the HRR, THR SPR, and SF values, but also delays the TTI of the samples, improving the fire safety of TPU. The SEM results show that the density of residue of TPU-2 and TPU-1 is better than TPU-0, so it can be seen

that the HGM-Fe₂O₃ is added into composites for promoting the charring with remarkable smoke suppression properties. In this process, this can protect the inner matrix and reduce the amount of combustible gas and smoke-forming materials in the gas phase during combustion.

The SDT results show that iron compound can promote the formation of carbon dioxide at last stage; this can be confirmed by the results of TG-IR. Combined with mass curve, there is a certain mass loss after the formation of carbon layer. And HGM-Fe₂O₃ can reduce the release of aliphatic hydrocarbons and CO from TPU composites during combustion process, and improve the fire safety of TPU.

Acknowledgements The authors gratefully acknowledge the National Natural Science Foundation of China (No. 51106078, No. 51206084), the University Research and Development Projects Shandong Province (J14LA13), and the Major Special Projects of Science and Technology from Shandong Province (2015ZDZX11011).

References

- Bocz K, Bárány T, Toldy A, Bodzay B, Csontos I, Madi K, Marosi G. Self-extinguishing polypropylene with a mass fraction of 9% intumescent additive—a new physical way for enhancing the fire retardant efficiency. *Polym Degrad Stab.* 2013;98:79–86.
- Li X, Yang B. Synergistic effects of pentaerythritol phosphate nickel salt (PPNS) with ammonium polyphosphate in flame retardant of polyethylene. *J Therm Anal Calorim.* 2015;122:359–68.
- Deodhar S, Shanmuganathan K, Fan Q, Wilkie CA, Costache MC, Dembsey NA, Patra PK. Calcium carbonate and ammonium polyphosphate-based flame retardant composition for polypropylene. *J Appl Polym Sci.* 2011;120:1866–73.
- Chen XL, Ma CY, Jiao CM. Synergistic effects between iron-graphene and ammonium polyphosphate in flame-retardant thermoplastic polyurethane. *J Therm Anal Calorim.* 2016. doi:10.1007/s10973-016-5494-7.
- Wang W. Fabrication of carbon black coated flexible polyurethane foam for significantly improved fire safety. *RSC Adv.* 2015;5:55870–8.
- Tabuani D, Bellucci F, Terenzi A, Camino G. Flame retarded thermoplastic polyurethane (TPU) for cable jacketing application. *Polym Degrad Stab.* 2012;97:2594–601.
- Chen XL, Zhuo JL, Jiao CM. Thermal degradation characteristics of flame retardant polylactide using TG-IR. *Polym Degrad Stab.* 2012;97:2143–7.
- Apaydin K, Laachachi A, Ball V, Jimenez M, Bourbigot S, Toniazzo V, Ruch D. Polyallylamine–montmorillonite as super flame retardant coating assemblies by layer-by-layer deposition on polyamide. *Polym Degrad Stab.* 2013;98:627–34.
- Chen Y, Peng H, Li J, Xia Z, Tan H. A novel flame retardant containing phosphorus, nitrogen, and sulfur. *J Therm Anal Calorim.* 2014;115:1639–49.
- Chen L, Wang YZ. A review on flame retardant technology in China. Part I: development of flame retardants. *Polym Adv Technol.* 2009;21:1–26.
- Wang N, Xu G, Wu Y, et al. The influence of expandable graphite on double-layered microcapsules in intumescent flame-retardant natural rubber composites. *J Therm Anal Calorim.* 2015;123:1–13.
- Hsiue GH, Liu YL, Tsiao J. Phosphorus-containing epoxy resins for flame retardancy V: synergistic effect of phosphorus–silicon on flame retardancy. *J Appl Polym Sci.* 2000;78:1–7.
- Serge B, Verhart DL, Gilman JW, Awad WH, Davis RD, Morgan AB, Wilkie CA. Investigation of nanodispersion in polystyrene–montmorillonite nanocomposites by solid-state NMR. *J Polym Sci Polym Phys.* 2003;41:3188–213.
- Lin M, Li B, Li Q, Li S, Zhang S. Synergistic effect of metal oxides on the flame retardancy and thermal degradation of novel intumescent flame-retardant thermoplastic polyurethanes. *J Appl Polym Sci.* 2011;121:1951–60.
- Tidjani A, Wilkie CA. Photo-oxidation of polymeric-inorganic nanocomposites: chemical, thermal stability and fire retardancy investigations. *Polym Degrad Stab.* 2001;74:33–7.
- Dalai S, Vijayalakshmi S, Shrivastava P, Sivam SP, Sharma P. Preparation and characterization of hollow glass microspheres (HGMs) for hydrogen storage using urea as a blowing agent. *Microelectron Eng.* 2014;126:65–70.
- Liu L, Hu J, Zhuo JL, Jiao CM, Chen XL, Li SX. Synergistic flame retardant effects between hollow glass microspheres and magnesium hydroxide in ethylene-vinyl acetate composites. *Polym Degrad Stab.* 2014;104:87–94.
- Sun L, Qu Y, Li S. Co-microencapsulate of ammonium polyphosphate and pentaerythritol in intumescent flame-retardant coatings. *J Therm Anal Calorim.* 2012;111:1099–106.
- Devi RR, Maji TK. In situ polymerized wood polymer composite: effect of additives and nanoclay on the thermal, mechanical properties. *Mater Res.* 2013;16:954–63.
- Chen XL, Jiang YF, Jiao CM. Synergistic effects between hollow glass microsphere and ammonium polyphosphate on flame-retardant thermoplastic polyurethane. *J Therm Anal Calorim.* 2014;117:857–66.
- Bentjen SB, Nelson DA, Tarasevich BJ, Rieke PC. The introduction of alkyl, ester, carboxylate, amino, hydroxyl, and phosphate functional groups to the surface of polyethylene. *J Appl Polym Sci.* 1992;44:965–80.
- You Z, Liu GS, Jian-Xin DU. Influencing mechanism of transition metal oxide on thermal decomposition of ammonium polyphosphate. *Chin J Inorg Chem.* 2013;29:1115–22.
- Carty P, Docherty A. Iron-containing compounds as flame retarding/smoke-suppressing additives for PVC. *Fire Mater.* 1988;12:109–13.
- Du SL, Lin XB, Jian RKM, Deng C, Wang YZ. Flame-retardant wrapped ramie fibers towards suppressing “candlewick effect” of polypropylene/ramie fiber composites. *Chin J Polym Sci.* 2014;33:84–94.
- Carty P, White S. The effect of temperature on char formation in polymer blends: an explanation of the role of the smoke suppressant FeOOH acting in ABS/CPVC polymer blends. *Polym Degrad Stab.* 2002;75:173–84.
- Peng HQ, Zhou Q, Wang DY, Chen L, Wang YZ. A novel charring agent containing caged bicyclic phosphate and its application in intumescent flame retardant polypropylene systems. *J Ind Eng Chem.* 2008;14:589–95.
- Zhou K. Synergetic effect of ferrocene and MoS₂ in polystyrene composites with enhanced thermal stability, flame retardant and smoke suppression properties. *RSC Adv.* 2014;4:13205–14.
- Chen XL, Jiang YF, Jiao CM. Smoke suppression properties of ferrite yellow on flame retardant thermoplastic polyurethane based on ammonium polyphosphate. *J Hazard Mater.* 2014;266:114–21.
- Ricciardi MR, Antonucci V, Zarrelli M, Giordano M. Fire behavior and smoke emission of phosphate-based inorganic fire-retarded polyester resin. *Fire Mater.* 2012;36:203–15.
- Duquesne S, Bras ML, Bourbigot S, Delobel R, Camino G, Eling B, Lindsay C, Roels T. Thermal degradation of polyurethane and polyurethane/expandable graphite coatings. *Polym Degrad Stab.* 2001;74:493–9.
- Gui H. Synergistic effect of graphene and an ionic liquid containing phosphonium on the thermal stability and flame retardancy of polylactide. *RSC Adv.* 2015;5:27814–22.
- Marney DCO, Russell LJ, Mann R. Fire performance of wood (*Pinus radiata*) treated with fire retardants and a wood preservative. *Fire Mater.* 2008;32:357–70.
- Zhao L. Novel tough and thermally stable cyanate ester resins with high flame retardancy, low dielectric loss and constant based on a phenolphthalein type polyarylether sulfone. *RSC Adv.* 2015;5:58989–9002.
- Schartel B, Hull TR. Development of fire-retarded materials—interpretation of cone calorimeter data. *Fire Mater.* 2007;31:327–54.
- Yang H, Song L, Tai Q, Wang X, Yu B, Yuan Y, Hu Y, Yuen RKK. Comparative study on the flame retarded efficiency of melamine phosphate, melamine phosphite and melamine hypophosphite on poly(butylene succinate) composites. *Polym Degrad Stab.* 2014;105:248–56.